Journal of Data Science and Modeling, Vol. 3, No. 2, 45-68, June 2025

Research Manuscript

Lognormal structured additive regression model for spatio-temporal data and its application to breast cancer data in Iran

Hasti Hashemi [1], Mahmoud Mirjalili[2], Soudabe Sajjadipanah[3] *

[1]Department of Statistics, Science and Research Branch, Islamic Azad University, Tehran, Iran,

[2]Department of Statistics, Velayat University, Velayat, Iran,

[3] University of Applied Science and Technology, Tangestan Branch, Tangestan, Iran.

Recieved: 04/10/2025 Accepted: 03/08/2026

Abstract: Medical data are typically recorded across geographic regions and over successive time points, giving rise to spatio-temporal structures that present important statistical modelling challenges. In this study, we propose a spatio-temporal regression model based on the lognormal distribution within the structured additive regression framework. The lognormal assumption accommodates the positive skewness and heteroscedasticity of the incidence-rate data. Bayesian inference for the model parameters was conducted using the integrated nested Laplace approximation (INLA), which delivers substantial computational gains over Markov chain Monte Carlo methods while maintaining comparable accuracy. We systematically compared four types of spatio-temporal interactions (Types I–IV) to identify the most parsimonious and best-fitting dependence structure. To evaluate performance, we applied the proposed model and several competitors to breast cancer incidence data from all provinces of Iran over the period 2010–2019. The results demonstrated the clear superiority of the lognormal structured additive regression (LNSTAR) model, with the Type II (temporal-only) interaction providing the best fit. Beyond its methodological contribution, this analysis provides actionable risk stratification to inform targeted screening policies in Iran.

Keywords: Bayesian inference, Breast cancer, Integrated nested Laplace approximation, Lognormal structured additive regression model, Spatio-temporal interaction. **Mathematics Subject Classification (2010):** 62M30, 62F15, 62P10.

*soodabesajadi@yahoo.com

1. Introduction

The analysis of spatio-temporal data plays a pivotal role in shaping health, economic, and population policies. As Utazi et al. (2018) emphasized, such analyses seek to characterize both local and global variations in spatial patterns over time and to quantify the associated relationships. Regression models provide a natural framework for this analysis. In recent decades, there has been considerable interest in modelling health data, with cancer registries representing a particularly active area of application. Bayesian regression models—incorporating both spatial and spatio-temporal structures—have emerged as a standard tool in this context; for a comprehensive discussion, see Greenland (2006), Berry et al. (2011), and Baio (2012). The Bayesian paradigm offers the flexibility to encode prior scientific knowledge and to decompose complex hierarchical models into simpler conditional components. However, its principal practical obstacle lies in computational intractability, as posterior distributions and associated summary quantities seldom admit closed forms. Sampling-based algorithms, most notably Markov chain Monte Carlo (MCMC), circumvent this difficulty by generating draws from the posterior, and dedicated software packages, such as BayesX Lang et al. (2005), OpenBUGS Lunn et al. (2009), Stan Gelman et al. (2015), and various R implementations, have made these methods widely accessible.

Despite their flexibility, MCMC algorithms face formidable challenges when applied to complex spatio-temporal models. Achieving adequate convergence rates can be exceedingly time-consuming and can undermine computational efficiency. To address this, Rue et al. (2009) proposed the integrated nested Laplace approximation (INLA), which delivers substantial speed gains while retaining accuracy comparable to that of MCMC. INLA is specifically tailored to latent Gaussian models, a class encompassing a broad range of spatial and spatio-temporal specifications, and has accordingly found extensive application Riebler et al. (2012); Li et al. (2012); Blangiardo et al. (2013).

The specific case of breast cancer surveillance in Iran illustrates both the promise and limitations of current practices. Faramarzi et al. (2024) provided a valuable descriptive atlas of multiple cancers at the county level using scan statistics and local Moran's I. However, their purely frequentist approach precluded covariate adjustment and neglected temporal dynamics, leaving the drivers of the observed clusters largely unexplored. Hashemi et al. (2024) adopted a Bayesian BYM specification to incorporate ecological factors, such as obesity and physical activity. Their analysis remained confined to coarse provincial aggregation and a narrow five-year window (2005–2009). Their reliance on MCMC introduces computational bottlenecks and convergence concerns that limit the exploration of richer dependence structures.

The most recent advance, by Rahimzadeh et al. (2025), represents a major step forward: they provided district-level Bayesian estimates for breast cancer risk in Iran across 22 years (2000–2021), revealing striking subnational heterogeneity and a pronounced education gradient, plausibly attributable to differential diagnostic access. Closer inspection of their model, however, identifies three notable limitations. One is that the temporal component was specified as exchangeable (unstructured), failing to capture smooth, autocorrelated trends characteristic of chronic disease. Another concerns the absence of any spatio-temporal interaction term, effectively assuming that spatial disparities remain fixed over time—an assumption that is frequently untenable. A third issue lies in the substantial computational demands of MCMC with 316 spatial units, which may preclude exhaustive model comparisons and sensitivity assessments.

These collective gaps motivate a modelling framework that is both computationally efficient and inferentially flexible, capable of simultaneously accommodating: (a) continuous incidence rates to stabilise variance and permit direct covariate interpretation on the rate scale; (b) structured temporal evolution (e.g., random walks of order 1 or 2) to reflect the inertia in cancer trends; (c) the full spectrum of spatio-temporal interactions (Types I–IV; see Knorr-Held, 2000) to determine whether disparities are amplifying or attenuating over time; and (d) Bayesian inference via INLA to reduce computational overhead while maintaining accuracy.

The present study introduces precisely such a framework: a Lognormal Structured Additive Regression (LNSTAR) model for spatio-temporal disease mapping. By combining a lognormal response with structured additive predictors—encompassing BYM2 spatial effects, RW1/RW2 temporal effects, and all four interaction types—our proposal extends existing work in four specific directions: (i) it represents the first LNSTAR application to breast cancer incidence in Iran; (ii) it updates the temporal window to the most recent decade (2010–2019); (iii) it integrates a richer set of lifestyle and environmental covariates, previously discussed only qualitatively; and (iv) it systematically compares the four interaction types via the Deviance Information Criterion (DIC), identifying the most plausible dependence structure. Beyond its methodological contribution, the analysis provides actionable risk stratification to inform targeted screening policies, thereby complementing and refining the district-level disparities documented by Rahimzadeh et al. (2025).

The remainder of this paper is organized as follows. Section 2 introduces the lognormal regression model. Section 3 develops the lognormal structured additive regression model for spatio-temporal data. Section 4 presents Bayesian inference for the proposed model parameters. Section 5 applies our model and several competitors to breast cancer incidence data from Iranian provinces over 2010–2019.

Section 6 presents the conclusions and discusses directions for future research.

2. Lognormal Regression Model

Let Z be a normally distributed random variable with mean μ_z and variance $1/\tau_z$, where $\tau_z > 0$ is the precision parameter. Then, $Y = \exp(Z)$ follows a lognormal distribution, denoted by $\mathrm{LN}(\mu_z, \tau_z)$, with density function

$$f_Y(y) = \frac{\sqrt{\tau_z}}{y\sqrt{2\pi}} \exp\left\{-\frac{\tau_z}{2}(\ln y - \mu_z)^2\right\}, \quad y > 0,\ \mu_z \in \mathbb{R}. \tag{2.1}$$

Moreover, $\mathrm{E}[Y] = \exp(\mu_z + 1/(2\tau_z))$ and $\mathrm{Var}[Y] = (\exp(1/\tau_z) - 1)\exp(2\mu_z + 1/\tau_z)$.

To formulate a regression model, we condition the distribution of Y on a vector of covariates $\boldsymbol{x}$. Let Y_i, $i = 1, \ldots, n$, be independent responses. We assume that the conditional expectation of $Z_i = \ln Y_i$ is a linear function of the covariates:

$$\mathrm{E}[Z_i \mid \boldsymbol{x}_i; \boldsymbol{\beta}] = \beta_0 + \beta_1 x_{i1} + \ldots + \beta_p x_{ip} = \boldsymbol{x}_i'\boldsymbol{\beta}, \quad i = 1, \ldots, n,$$

where $\boldsymbol{\beta} = (\beta_0, \ldots, \beta_p)'$ is the vector of regression coefficients and $\boldsymbol{x}_i = (1, x_{i1}, \ldots, x_{ip})'$. It follows from the properties of the lognormal distribution that

$$\mathrm{E}[Y_i \mid \boldsymbol{x}_i; \boldsymbol{\beta}, \tau_z] = \exp\left\{\boldsymbol{x}_i'\boldsymbol{\beta} + \frac{1}{2\tau_z}\right\}, \quad i = 1, \ldots, n.$$

Thus, we write

$$Y_i \mid \boldsymbol{x}_i; \boldsymbol{\beta}, \tau_z \sim \mathrm{LN}(\boldsymbol{x}_i'\boldsymbol{\beta}, \tau_z).$$

Given observed data $\boldsymbol{y} = (y_1, \ldots, y_n)'$ and covariate matrix $\boldsymbol{X} = (\boldsymbol{x}_1, \ldots, \boldsymbol{x}_n)'$, the likelihood is

$$L(\boldsymbol{\beta}, \tau_z \mid \boldsymbol{x}, \boldsymbol{y}) = \left(\frac{\tau_z}{2\pi}\right)^{n/2} \frac{\exp\left\{-\frac{\tau_z}{2}\sum_{i=1}^{n}(\ln y_i - \boldsymbol{x}_i'\boldsymbol{\beta})^2\right\}}{\prod_{i=1}^{n} y_i}.$$

The likelihood is nonlinear in the parameters $\boldsymbol{\beta}$ and τ_z; closed-form maximum likelihood estimators are not available. Consequently, numerical optimisation—or, as we adopt here, Bayesian inference via INLA—is required for parameter estimation.

3. Lognormal Structured Additive Regression Model

Fahrmeir et al. (2004) introduced a broad class of structured additive regression (STAR) models, which encompass several important subclasses as special cases. STAR models are flexible and accommodate the smooth effects of continuous covariates, as well as temporal and spatial dependence structures. We now define

a lognormal spatio-temporal model within this framework, denoted the LNSTAR model.

Let Y_{st}, $s = 1, \ldots, S$, $t = 1, \ldots, T$, be a continuous response variable in region s at time t. Let $Z_{st} = \ln Y_{st}$. We specify the additive predictor for the conditional mean of Z_{st} as

$$\begin{aligned} \mu_{st} &= \mathrm{E}[Z_{st} \mid \boldsymbol{x}_{st}; \boldsymbol{\beta}, \tau_z, \phi_s^*, \gamma_t^*, \delta_{st}] \\ &= \boldsymbol{x}_{st}'\boldsymbol{\beta} + \phi_s^* + \gamma_t^* + \delta_{st} + \boldsymbol{f}(\boldsymbol{z}_{st}), \end{aligned} \tag{3.2}$$

for $s = 1, \ldots, S$ and $t = 1, \ldots, T$, where

- $\boldsymbol{x}_{st}$ is the vector of covariates with associated fixed effects $\boldsymbol{\beta} = (\beta_0, \ldots, \beta_p)'$;
- ϕ_s^* is the combined spatial effect, decomposed into structured and unstructured components;
- γ_t^* is the combined temporal effect, decomposed analogously;
- δ_{st} is the spatio-temporal interaction effect;
- $\boldsymbol{f}(\boldsymbol{z}_{st}) = (f_1(z_{st}), \ldots, f_k(z_{st}))$ captures smooth, nonlinear effects of continuous covariates.

The conditional expectation of Y_{st} is then

$$\mathrm{E}[Y_{st} \mid \boldsymbol{x}_{st}; \boldsymbol{\beta}, \tau_z, \phi_s^*, \gamma_t^*, \delta_{st}] = \exp\left(\mu_{st} + \frac{1}{2\tau_z}\right), \quad s = 1, \ldots, S, \ t = 1, \ldots, T, \tag{3.3}$$

and the conditional density of Y_{st} is

$$f_{Y_{st}}(y_{st} \mid \mu_{st}, \tau_z) = \frac{\sqrt{\tau_z}}{y_{st}\sqrt{2\pi}} \exp\left\{-\frac{\tau_z}{2}(\ln y_{st} - \mu_{st})^2\right\}, \quad y_{st} > 0, \ s = 1, \ldots, S, \ t = 1, \ldots, T. \tag{3.4}$$

According to Cressie and Wikle (2011), certain stochastic processes are used to describe the latent spatial, temporal, and spatio-temporal effects. In the following subsections, we review these processes in detail.

3.1 Stochastic models for spatial and temporal effects

3.1.1 Spatial effect

In Equation (3.2), the combined spatial effect ϕ_s^* is a convolution of a structured spatial effect ϕ_s and an unstructured (exchangeable) spatial effect φ_s. Following Blangiardo and Cameletti (2015), we assume $\varphi_s \sim \mathrm{N}(0, \tau_\varphi^{-1})$ for $s = 1, \ldots, S$, independently across regions, where τ_φ is a precision parameter.

For the structured spatial effect ϕ_s, we employ the intrinsic conditional autoregressive (ICAR) prior Besag et al. (1991), a limiting case of the proper CAR model with spatial correlation parameter $\rho_\phi = 1$. Let $\boldsymbol{\phi} = (\phi_1, \ldots, \phi_S)'$. The ICAR prior is specified conditionally as

$$\phi_s \mid \boldsymbol{\phi}_{-s}, \tau_\phi, \rho_\phi \sim \mathrm{N}\left(\sum_{\ell=1}^{S} \frac{w_{s\ell}\phi_\ell}{w_{s+}},\ \rho_\phi(\tau_\phi w_{s+})^{-1} \right), \quad s = 1, \ldots, S,$$

where $w_{s\ell}$ are spatial adjacency weights, $w_{s+} = \sum_{\ell=1}^{S} w_{s\ell}$, and $\tau_\phi > 0$ is a precision parameter. Typically, we set

$$w_{s\ell} = \begin{cases} 1, & \text{if regions } s \text{ and } \ell \text{ are neighbors,} \\ 0, & \text{if } s = \ell, \text{ or if regions } s \text{ and } \ell \text{ are not neighbors.} \end{cases}$$

This specification yields the improper joint density

$$\pi(\boldsymbol{\phi} \mid \tau_\phi) \sim \tau_\phi^{(S-1)/2} \exp\left\{ -\frac{\tau_\phi}{2} \boldsymbol{\phi}' \mathbb{A}_\phi \boldsymbol{\phi} \right\},$$

where $\mathbb{A}_\phi = \mathbb{D} - \mathbb{W}$ is the $S \times S$ precision matrix, $\mathbb{D} = \mathrm{diag}(w_{1+}, \ldots, w_{S+})$, and $\mathbb{W} = [w_{s\ell}]$. The ICAR prior is improper because $\mathbb{A}_\phi$ has rank $S-1$; identifiability is achieved by imposing the sum-to-zero constraint $\sum_{s=1}^{S} \phi_s = 0$. For further details on CAR and ICAR models in spatial epidemiology, see Besag (1974), Besag et al. (1991), Cressie (1993), Cressie and Chen (1989), and Cressie and Wikle (2011).

3.1.2 Temporal effect

The combined temporal effect γ_t^* in Equation (3.2) is the sum of a structured temporal effect γ_t and an unstructured temporal effect ν_t:

$$\nu_t \sim \mathrm{N}(0, \tau_\nu^{-1}), \quad t = 1, \ldots, T,$$

independently across time. For the structured temporal effect, following Luan et al. (2016), we adopt either the random walk of order 1 (RW1) prior,

$$\gamma_t \mid \gamma_{t-1} \sim \mathrm{N}(\gamma_{t-1}, \tau_\gamma^{-1}), \quad t = 2, \ldots, T,$$

or the random walk of order 2 (RW2) prior,

$$\gamma_t \mid \gamma_{t-1}, \gamma_{t-2} \sim \mathrm{N}(2\gamma_{t-1} - \gamma_{t-2}, \tau_\gamma^{-1}), \quad t = 3, \ldots, T,$$

with appropriate initial conditions. The RW1 prior induces a smooth, locally linear trend, while RW2 induces an even smoother, locally quadratic trend. In the INLA framework, both priors are computationally tractable and are preferred to ICAR for temporal effects due to their natural ordering and ease of interpretation. These priors are also used to model the nonlinear effects of continuous covariates $\boldsymbol{f}(\cdot)$ in Equation (3.2).

3.1.3 Spatio-temporal interaction

Models that include only spatial or temporal effects are often inadequate for data exhibiting spatial structures that vary over time. To capture such dynamics, we incorporate an interaction term δ_{st} in Equation (3.2). Following the typology of Knorr-Held (2000), we consider four types of spatio-temporal interaction priors.

Let $\boldsymbol{\delta} = (\delta_{11}, \ldots, \delta_{ST})'$ denote the $ST \times 1$ vector of interaction effects.

- **Type-I spatio-temporal interaction:** The δ_{st} are independent and identically distributed, with no spatial or temporal structure:

$$\boldsymbol{\delta}_{ST} \mid \tau_\delta \sim \mathrm{N}(\mathbf{0}, \tau_\delta^{-1}\mathbb{I}),$$

  where τ_δ is a precision parameter and $\mathbb{I}$ is an identity matrix of dimension $ST \times ST$.

- **Type-II spatio-temporal interaction:** The interactions have a temporal structure but are independent across regions:

$$\boldsymbol{\delta}_{ST} \mid \tau_\delta \sim \mathrm{N}\big(\mathbf{0}, \tau_\delta^{-1}\mathbb{I} \otimes \mathbb{A}_\gamma\big)\,,$$

  where $\otimes$ denotes the Kronecker product, $\mathbb{I}$ is the $S \times S$ identity matrix, and $\mathbb{A}_\gamma$ is the $T \times T$ precision matrix of the temporal process (RW1 or RW2).

- **Type-III spatio-temporal interaction:** The interactions have a spatial structure but are independent across time:

$$\boldsymbol{\delta}_{ST} \mid \tau_\delta \sim \mathrm{N}\big(\mathbf{0}, \tau_\delta^{-1}\mathbb{A}_\phi \otimes \mathbb{I}\big)\,,$$

  where $\mathbb{I}$ is the $T \times T$ identity matrix and $\mathbb{A}_\phi$ is the spatial precision matrix defined in Subsection 3.1.1.

- **Type-IV spatio-temporal interaction:** The interactions exhibit both spatial and temporal structures:

$$\boldsymbol{\delta}_{ST} \mid \tau_\delta \sim \mathrm{N}\big(\mathbf{0}, \tau_\delta^{-1}\mathbb{A}_\phi \otimes \mathbb{A}_\gamma\big)\,,$$

  where $\mathbb{A}_\phi$ and $\mathbb{A}_\gamma$ were introduced in Subsections 3.1.1 and 3.1.2, respectively.

Type IV is the most complex and computationally demanding. In practice, model comparison criteria such as DIC can be used to select the most appropriate interaction type, as demonstrated in Section 5.

4. Bayesian Inference

Let $\boldsymbol{\xi} = (\phi_1^*, \ldots, \phi_S^*, \gamma_1^*, \ldots, \gamma_T^*, \delta_{11}, \ldots, \delta_{ST})'$ be the vector of latent effects of dimension $m = S + T + ST$, and let $\boldsymbol{\theta} = (\boldsymbol{\beta}', \tau_z, \tau_{\phi^*}, \tau_{\gamma^*}, \tau_\delta)'$ be the vector of hyperparameters. The marginal likelihood of the LNSTAR model is

$$L(\boldsymbol{\theta} \mid \mathcal{D}) = \int_{\mathbb{R}^m} f_{\boldsymbol{Y},\boldsymbol{\xi}}(\boldsymbol{y}, \boldsymbol{\xi} \mid \boldsymbol{\theta}) \, \mathrm{d}\boldsymbol{\xi}, \tag{4.5}$$

where $\mathcal{D}$ denotes the observed data and $f_{\boldsymbol{Y},\boldsymbol{\xi}}(\boldsymbol{y}, \boldsymbol{\xi} \mid \boldsymbol{\theta})$ is the joint density of the response vector and latent effects. The direct evaluation of (4.5) is impractical because of the high-dimensional integral and the complexity of the latent structure.

We adopt a Bayesian approach. Let $\boldsymbol{\Omega} = (\boldsymbol{\xi}', \boldsymbol{\theta}')'$ denote the full parameter vector. Assuming prior independence among components, the prior distribution factorises as

$$\pi(\boldsymbol{\Omega}) = \pi(\boldsymbol{\beta})\pi(\boldsymbol{\phi}_S^*)\pi(\boldsymbol{\gamma}_T^*)\pi(\boldsymbol{\delta}_{ST})\pi(\tau_z)\pi(\tau_{\phi^*})\pi(\tau_{\gamma^*})\pi(\tau_\delta),$$

where $\boldsymbol{\phi}_S^* = (\phi_1^*, \ldots, \phi_S^*)'$ and $\boldsymbol{\gamma}_T^* = (\gamma_1^*, \ldots, \gamma_T^*)'$. For the regression coefficients, we specify weakly informative Gaussian priors:

$$\boldsymbol{\beta} \sim \mathrm{N}_{p+1}(\mathbf{0}, 10^{-4}\mathbb{I}_{p+1}),$$

where $\mathbb{I}_{p+1}$ is the identity matrix of dimension $p + 1$.

For the combined spatial and temporal effects, we employ the BYM2 specification of Riebler et al. (2016). The BYM2 model is a reparameterized version of the Besag–York–Mollié (BYM) specification designed to enhance parameter interpretability. The BYM2 framework distinguishes between structured spatial effects and unstructured idiosyncratic noise through a single mixing parameter, which quantifies the proportion of variance attributed to spatial processes. This approach effectively mitigates the identifiability challenges inherent in traditional spatial models and provides more stable estimation of spatial dependencies through the use of penalized complexity (PC) priors. This parameterisation represents the combined effect as

$$\phi_S^* = \frac{1}{\sqrt{\tau_{\phi^*}}} \left(\sqrt{1 - \rho_{\phi^*}} \, \upsilon_S + \sqrt{\rho_{\phi^*}} \, \phi_S \right),$$

where $\rho_{\phi^*} \in [0, 1]$ controls the proportion of variance attributable to the structured component, and τ_{ϕ^*} is the marginal precision of ϕ_S^*. The parameter $\rho_{\phi^*} = 0$ corresponds to pure unstructured variation, while $\rho_{\phi^*} = 1$ corresponds to pure structured spatial variation. The temporal combined effect γ_T^* is parameterised analogously.

For the precision parameters τ_z, τ_{ϕ^*}, τ_{γ^*}, and τ_δ, we adopt the penalised complexity (PC) priors of Simpson et al. (2017). The PC prior for a precision parameter τ is defined by the density

$$\pi(\tau) = \frac{1}{2}\tau^{-3/2}\exp\{-\lambda\tau^{-1/2}\}, \qquad \lambda = -\frac{\ln\alpha}{q},$$

where $q > 0$ and $0 < \alpha < 1$. The parameters have a direct interpretation: $P(\tau < q) = \alpha$. Thus, the user can encode a prior belief about the scale of the precision; for example, choosing $q = 1$ and $\alpha = 0.01$ implies that we a priori believe there is only a 1% probability that the precision is less than 1, reflecting a preference for moderate-to-high precision. This prior specification is attractive because it shrinks towards a simpler base model (infinite precision, i.e., zero variance) in a principled way. In this study, we set PC$(1, 0.01)$ for all precision parameters.

We perform Bayesian inference using the INLA methodology of Rue et al. (2009). INLA targets the marginal posterior distributions of the latent variables and hyperparameters as follows:

$$\tilde{\pi}(\xi_i \mid \mathcal{D}) \quad = \quad \int \tilde{\pi}(\xi_i \mid \boldsymbol{\theta}, \mathcal{D})\tilde{\pi}(\boldsymbol{\theta} \mid \mathcal{D})\,\mathrm{d}\boldsymbol{\theta}, \quad i = 1, \ldots, m,$$

for each latent effect ξ_i, and

$$\tilde{\pi}(\theta_j \mid \mathcal{D}) \quad = \quad \int \tilde{\pi}(\boldsymbol{\theta} \mid \mathcal{D})\,\mathrm{d}\boldsymbol{\theta}_{-j}, \quad j = 1, \ldots, \dim(\boldsymbol{\theta}),$$

for each hyperparameter θ_j, where $\boldsymbol{\theta}_{-j}$ denotes the vector $\boldsymbol{\theta}$ with the jth element omitted. INLA constructs nested Laplace approximations. The marginal posterior of the hyperparameters is approximated by

$$\tilde{\pi}(\boldsymbol{\theta} \mid \mathcal{D}) \quad \propto \quad \left.\frac{\pi(\boldsymbol{\eta}, \boldsymbol{\theta}) f(\boldsymbol{y} \mid \boldsymbol{\eta})}{\tilde{\pi}_G(\boldsymbol{\eta} \mid \boldsymbol{\theta}, \mathcal{D})}\right|_{\boldsymbol{\eta} = \boldsymbol{\eta}^*(\boldsymbol{\theta})},$$

where $\tilde{\pi}_G(\boldsymbol{\eta} \mid \boldsymbol{\theta}, \mathcal{D})$ is a Gaussian approximation to the full conditional distribution of the latent effects, and $\boldsymbol{\eta}^*(\boldsymbol{\theta})$ is the mode of this conditional distribution. The marginal posterior of each latent effect is then obtained via numerical integration over the hyperparameters:

$$\tilde{\pi}(\eta_i \mid \mathcal{D}) \quad = \quad \sum_k \tilde{\pi}(\eta_i \mid \boldsymbol{\theta}_k, \mathcal{D})\tilde{\pi}(\boldsymbol{\theta}_k \mid \mathcal{D})\Delta_k,$$

where the sum is taken over integration points $\boldsymbol{\theta}_k$ with weights Δ_k. For a full exposition of INLA, we refer to Rue et al. (2009) and Gómez-Rubio (2020).

5. Application to Breast Cancer Data

5.1 Data Description

We apply the proposed LNSTAR model to provincial-level incidence-rate data for breast cancer in Iran. The data were obtained from the Iranian National Cancer Registry System, maintained by the Ministry of Health and Medical Education, and cover the period 2010–2019. The study includes all 31 provinces of Iran. The response variable is the age-standardised incidence rate of breast cancer per 100,000 women, restricted to the female population aged 30 years and older. This rate is treated as a continuous outcome, consistent with the lognormal modelling framework.

The following covariates were selected based on their established or hypothesised associations with breast cancer risk and on data availability at the provincial level:

- Smoke: Average percentage of the adult female population reporting daily tobacco use. Source: Iranian National Health Survey (NHS).
- Redmeat: Average per capita consumption of red meat (grams per day). Source: Household Expenditure and Income Survey (HEIS).
- Sugar: Average per capita sugar consumption (grams per day). Source: HEIS.
- Literacy: Female literacy rate, defined as the percentage of women aged 15 years and above who are literate. Source: National Census.
- Dairy: Average per capita dairy-product consumption (grams per day). Source: HEIS.
- Age: Mean age of the female population aged 30 years and above. Source: National Census.
- VitaminD: Mean serum vitamin D level (nmol/L), estimated from provincial surveys. Source: Non-Communicable Diseases Research Centre (NCDRC).
- Humidity: Annual average relative humidity. Source: Iranian Meteorological Organisation.
- Temperature: Annual average temperature (°C). Source: Iranian Meteorological Organisation.

5.2 Model Specification

The following structured additive predictor was specified for the log-transformed incidence rate:

$$\begin{aligned}\mu_{st} &= \beta_0 + \beta_1(\text{Smoke}) + \beta_2(\text{Redmeat}) + \beta_3(\text{Sugar}) + \beta_4(\text{Literacy}) + \beta_5(\text{Dairy}) \\ &\quad + f_1(\text{Age}) + f_2(\text{VitaminD}) + f_3(\text{Humidity}) + f_4(\text{Temperature}) \\ &\quad + \phi_s^* + \gamma_t^* + \delta_{st}, \end{aligned} \tag{5.6}$$

for $s = 1, \ldots, 31$ and $t = 1, \ldots, 10$. The variables Smoke, Redmeat, Sugar, Literacy, and Dairy enter the model linearly, as there is no established evidence suggesting nonlinear relationships for these factors in the context of breast cancer incidence. In contrast, the variables Age, VitaminD, Humidity, and Temperature were treated nonlinearly using RW2 priors, allowing the data to determine the functional form; this is motivated by the potential for nonlinear dose–response relationships between environmental and demographic factors and breast cancer risk. The spatial effect ϕ_s^* follows the BYM2 specification with an ICAR prior for the structured component; the temporal effect γ_t^* follows the BYM2 specification with an RW1 prior; and δ_{st} is one of the four spatio-temporal interaction types defined in Subsection 3.1.3.

5.3 Model Comparison and Selection

To evaluate the performance of the LNSTAR model against competing specifications, we fitted four distributional models within the STAR framework: Gamma, Skew-Normal, Lognormal (LNSTAR), and Gaussian. For each distributional assumption, all four spatio-temporal interaction types (I–IV) were implemented. Model fit was assessed using the Deviance Information Criterion (DIC) Spiegelhalter et al. (2002), where lower values indicate a better balance between model fit and complexity. The results are summarized in Table 1.

The LNSTAR model consistently outperformed all competitors across all interaction types, as evidenced by its substantially lower DIC values. Within the LNSTAR framework, Type II (temporal structure only) and Type IV (both spatial and temporal structures) yielded the best fits, with DIC values of 585.419 and 589.681, respectively. The minimal difference between these two (4.262) suggests that the inclusion of spatial structure in the interaction term does not materially improve the model's explanatory power over a temporal-only interaction for this dataset. Conversely, Type I (unstructured) and Type III (spatial-only) interactions were markedly inferior, with DIC values for the lognormal case exceeding 1,280 and 1,590, respectively. These results indicate that the temporal dimension

of the interaction is the dominant source of variation in breast cancer incidence trends across Iranian provinces.

Based on these findings, we report the Bayes estimators (posterior means) and 95% credible intervals (CIs) for the Type II and Type IV specifications in Tables 2 and 4. From the results in these tables, the 95% CIs for β_{Redmeat} and β_{Sugar} include zero, indicating that these covariates are not statistically significant predictors of breast cancer incidence in this context. In contrast, the effects of tobacco use (Smoke) and dairy consumption (Dairy) are significantly positive. Furthermore, the literacy rate (Literacy) shows a significant positive association, likely reflecting better diagnostic access and health-seeking behavior among more educated populations.

To examine spatial dynamics, the Bayes estimators of the spatial effects for all models are mapped in Figure 1. The spatial patterns consistently indicate that northern and central provinces exhibit higher breast cancer incidence rates compared to eastern provinces. Temporal trends, illustrated in Figure 2, reveal a steady, linearly increasing trend in incidence over the ten-year study period (2010–2019). Finally, Figures 3–6 display the estimated spatio-temporal interactions and the predicted incidence rates for the Type II and Type IV LNSTAR models, providing a comprehensive visualization of the disease's evolution in Iran.

Table 1: DIC criterion for the evaluated models and four types of spatio-temporal interaction.

	Model			
Interaction	Gamma	Skew-Normal	Lognormal	Gaussian
Type I	1713.066	8009.043	1280.412	7140.307
Type II	1360.005	6149.942	**585.419**	6084.058
Type III	1725.325	–	1592.803	8147.252
Type IV	1363.631	6046.289	**589.681**	6076.719

6. Discussion

In this paper, we introduced the lognormal structured additive regression (LNSTAR) model for spatio-temporal disease mapping and demonstrated its application to breast cancer incidence data in Iran (2010–2019). Our results establish several principal findings regarding model performance, dependence structures, and epidemiologic drivers.

Table 2: Bayes estimators and 95% credible intervals for models incorporating Type II spatio-temporal interactions.

Model	Parameters	Bayes Estimation	Credible Interval
Lognormal	β_0	0.7548	(0.4673, 1.0412)
	β_{Smoke}	0.0045	(0.0004, 0.0086)
	β_{Redmeat}	0.0228	(−0.0230, 0.0687)
	β_{Sugar}	−0.0291	(−0.0862, 0.0282)
	β_{Literacy}	0.0645	(0.0357, 0.0932)
	β_{Dairy}	0.2222	(0.1073, 0.3377)
	τ_{Age}	319.8710	(7.4021, 1969.83)
	τ_{VitaminD}	705.4501	(11.2570, 4555.85)
	τ_{Humidity}	387.3736	(9.4575, 2380.75)
	$\tau_{\text{Temperature}}$	2517.5460	(9.6610, 15578.26)
	τ_z	149894.8	(83102.28, 245839.1)
	τ_{ϕ^*}	1531.506	(14.5562, 9853.14)
	ρ_{ϕ^*}	0.3068	(0.0124, 0.8802)
	τ_{γ^*}	281.0009	(87.3462, 637.2966)
	ρ_{γ^*}	0.8900	(0.5119, 0.9983)
	τ_δ	4319.618	(3609.213, 5187.463)
Gamma	β_0	0.7370	(0.4488, 1.0249)
	β_{Smoke}	0.0060	(0.0013, 0.0107)
	β_{Redmeat}	0.0214	(−0.0279, 0.0706)
	β_{Sugar}	−0.0238	(−0.0858, 0.0385)
	β_{Literacy}	0.0628	(0.0340, 0.0916)
	β_{Dairy}	0.1858	(0.0568, 0.3173)
	τ_{Age}	392.6198	(8.9618, 2478.65)
	τ_{VitaminD}	721.4784	(11.2022, 4688.74)
	τ_{Humidity}	436.3102	(10.4797, 2729.86)
	$\tau_{\text{Temperature}}$	2442.059	(9.8865, 15475.77)
	τ_z	5639.598	(4478.19, 7004.35)
	τ_{ϕ^*}	1253.545	(13.6043, 8146.93)
	ρ_{ϕ^*}	0.3210	(0.0141, 0.8878)
	τ_{γ^*}	295.4016	(89.6666, 650.1906)
	ρ_{γ^*}	0.9516	(0.6972, 0.9999)
	τ_δ	4129.244	(3108.45, 5372.69)

Table 3: Table 2: Continued (Skew-Normal and Gaussian).

Model	Parameters	Bayes Estimation	Credible Interval
Skew-Normal	β_0	1.4584	(1.1290, 1.7874)
	β_{Smoke}	0.0333	(0.0262, 0.0404)
	β_{Redmeat}	0.3177	(0.2515, 0.3838)
	β_{Sugar}	0.4322	(0.3373, 0.5269)
	β_{Literacy}	0.1087	(0.0763, 0.1412)
	β_{Dairy}	3.2950	(2.8607, 3.7268)
	τ_{Age}	0.0364	(0.3606, 0.0367)
	τ_{VitaminD}	42.7267	(42.1826, 43.3738)
	τ_{Humidity}	∞	$(0, \infty)$
	$\tau_{\text{Temperature}}$	47.2811	(45.3378, 51.0969)
	τ_z	2334.412	(2331.11, 2337.69)
	τ_{ϕ^*}	0.1569	(0.1565, 0.1573)
	ρ_{ϕ^*}	0.4863	(0.4702, 0.5027)
	τ_{γ^*}	7.0009	(6.7725, 7.2330)
	ρ_{γ^*}	0.7688	(0.7680, 0.7696)
Gaussian	β_0	-40.8962	$(-8176.96, 8088.34)$
	β_{Smoke}	-0.0884	$(-0.1478, -0.0291)$
	β_{Redmeat}	0.6281	$(-0.2012, 1.4568)$
	β_{Sugar}	0.0708	$(-0.9055, 1.0463)$
	β_{Literacy}	0.0282	$(-62.700, 62.705)$
	β_{Dairy}	12.9947	(11.6147, 14.3738)
	τ_{Age}	1356.680	(1350.60, 2190.26)
	τ_{VitaminD}	94.4684	(93.9696, 146.022)
	τ_{Humidity}	67.6133	(67.4237, 67.7990)
	$\tau_{\text{Temperature}}$	64.2649	(64.0311, 94.8279)
	τ_z	25646.64	(25549.1, 30710.2)
	τ_{ϕ^*}	9.6258	(9.5439, 9.7156)
	ρ_{ϕ^*}	0.0060	(0.0059, 0.0061)
	τ_{γ^*}	2.0023	(1.9956, 2.2927)
	ρ_{γ^*}	0.2313	(0.2300, 0.3584)
	τ_δ	31.8646	(31.7501, 45.4330)

6.1 Model Performance and Distributional Choice

The LNSTAR model substantially outperforms competing specifications—including Gamma, Skew-Normal, and Gaussian models—across all spatio-temporal interaction types. The superiority of the lognormal assumption is expected, given the

Table 4: Bayes estimators and 95% credible intervals for models incorporating Type IV spatio-temporal interactions.

Model	Parameters	Bayes Estimation	Credible Interval
Lognormal	β_0	2.8430	$(-40.694, 46.343)$
	β_{Smoke}	0.0050	(0.0000, 0.0090)
	β_{Redmeat}	0.0540	$(-0.0150, 0.1230)$
	β_{Sugar}	-0.0720	$(-0.1500, 0.0070)$
	β_{Literacy}	-0.0750	$(-4.5850, 4.4310)$
	β_{Dairy}	0.2320	(0.0850, 0.3800)
	τ_{Age}	519.9410	(2.7170, 3584.32)
	τ_{VitaminD}	473.8800	(6.4790, 3163.79)
	τ_{Humidity}	748.6360	(5.1240, 5127.56)
	$\tau_{\text{Temperature}}$	547.3450	(3.6610, 3750.36)
	τ_z	143354	(76952, 237902)
	τ_{ϕ^*}	162.6130	(2.8420, 1034.12)
	ρ_{ϕ^*}	0.3500	(0.0300, 0.8860)
	τ_{γ^*}	304.2650	(104.227, 690.925)
	ρ_{γ^*}	0.8780	(0.5510, 0.9920)
	τ_δ	1063.477	(877.590, 1262.21)
Gamma	β_0	2.8440	$(-40.692, 46.343)$
	β_{Smoke}	0.0080	(0.0020, 0.0140)
	β_{Redmeat}	0.0410	$(-0.0400, 0.1220)$
	β_{Sugar}	-0.0730	$(-0.1640, 0.0180)$
	β_{Literacy}	-0.0780	$(-4.5870, 4.4280)$
	β_{Dairy}	0.1550	$(-0.0020, 0.3140)$
	τ_{Age}	1032.904	(4.7360, 6941.70)
	τ_{VitaminD}	1249.576	(4.7790, 8208.71)
	τ_{Humidity}	764.0390	(3.7860, 5180.63)
	$\tau_{\text{Temperature}}$	1335.411	(5.2330, 8767.59)
	τ_z	5504.848	(4356.74, 6846.58)
	τ_{ϕ^*}	1303.707	(2.3190, 7857.30)
	ρ_{ϕ^*}	0.3080	(0.0120, 0.9010)
	τ_{γ^*}	263.3250	(83.0720, 614.442)
	ρ_{γ^*}	0.9350	(0.6250, 1.0000)
	τ_δ	1199.014	(886.914, 1592.33)

positive skewness and heteroscedasticity characteristic of incidence rate data. The Gaussian model, which assumes symmetry and constant variance, is clearly in-

Table 5: Table 3: Continued (Skew-Normal and Gaussian).

Model	Parameters	Bayes Estimation	Credible Interval
Skew-Normal	β_0	4.9000	$(-38.664, 48.427)$
	β_{Smoke}	-0.0980	$(-0.1520, -0.0450)$
	β_{Redmeat}	0.8650	(0.1190, 1.6180)
	β_{Sugar}	0.0280	$(-0.8340, 0.8790)$
	β_{Literacy}	-0.2870	$(-4.7970, 4.2200)$
	β_{Dairy}	15.6150	(13.9730, 17.1010)
	τ_{Age}	0.0100	$(-0.0960, 0.1250)$
	τ_{VitaminD}	659.4810	(4.7510, 4513.42)
	τ_{Humidity}	869.1090	(5.3920, 5865.85)
	$\tau_{\text{Temperature}}$	995.8140	(5.7060, 6642.31)
	τ_z	28335.10	(4386.40, 94062.7)
	τ_{ϕ^*}	0.7320	(0.4180, 0.9210)
	ρ_{ϕ^*}	1587.953	(4.8880, 10658.0)
Gaussian	β_0	8.2040	(6.8750, 9.6930)
	β_{Smoke}	5.0450	$(-38.523, 48.577)$
	β_{Redmeat}	-0.0970	$(-0.1520, -0.0430)$
	β_{Sugar}	0.8910	(0.1190, 1.6610)
	β_{Literacy}	-0.0130	$(-0.8990, 0.8730)$
	β_{Dairy}	-0.2920	$(-4.8030, 4.2140)$
	τ_{Age}	28662.33	(4930.41, 87733.4)
	τ_{VitaminD}	1317.658	(4.0460, 8809.24)
	τ_{Humidity}	853.6750	(3.6740, 5853.20)
	$\tau_{\text{Temperature}}$	535.7050	(2.6010, 3684.76)
	τ_z	15.4420	(13.7190, 17.1040)
	τ_{ϕ^*}	0.9150	(0.4710, 1.0000)
	ρ_{ϕ^*}	458.8030	(1.3300, 3047.56)

adequate for these data, as reflected in its uniformly higher DIC values. This underscores the importance of selecting a distributional family that respects the support and skewness of the outcome. For continuous health outcomes with positive skew, the lognormal distribution offers a principled alternative to the Gaussian model and should be considered over ad hoc transformations.

6.2 Spatio-Temporal Interaction Selection

Within the LNSTAR framework, Type II (temporal-only) and Type IV (both spatial and temporal) interactions provide comparable fit. This suggests that the tem-

poral structure in the interaction term captures the majority of relevant variation, while the addition of spatial structure in the interaction provides marginal improvement. Practically, the Type II specification may be preferred due to its lower computational cost and simpler interpretation. This implies that when spatio-temporal dynamics are dominated by temporal evolution, simpler interaction types may suffice without sacrificing predictive accuracy.

6.3 Covariate Associations

We identified significant positive associations between breast cancer incidence and tobacco use, literacy, and dairy consumption. The positive literacy gradient echoes the findings of Rahimzadeh et al. (2025) and is likely driven by surveillance bias: women with higher education often have greater health awareness and diagnostic access. Future work should distinguish between diagnostic access and underlying biological risk by linking incidence data to cancer stage at diagnosis. The association with tobacco use reinforces the need for sustained tobacco control policies. While dairy consumption was significant, this may reflect residual confounding by other lifestyle factors, as mechanistic evidence linking dairy to breast cancer remains inconclusive.

6.4 Methodological Contributions and Computational Advantages

This study represents the first application of the LNSTAR framework to cancer incidence in Iran and the first to systematically compare all four spatio-temporal interaction types within the lognormal family. The use of INLA confers substantial computational advantages over MCMC, allowing the entire model-fitting procedure to be completed in minutes. This efficiency is critical for routine surveillance and for exploring complex model specifications across large spatial domains.

6.5 Policy Implications and Future Work

The findings suggest that targeted screening programs in high-risk provinces (e.g., Tehran, Isfahan, and Yazd) and among lower-literacy populations—where diagnostic access may be limited—could yield substantial health gains. Future work should incorporate additional covariates such as socioeconomic indicators and air pollution. Extending the LNSTAR framework to include spatially varying coefficients (SVC) would further elucidate the drivers of geographic heterogeneity.

Conclusion

The LNSTAR model provides a flexible, efficient, and rigorous framework for spatio-temporal disease mapping. By combining a lognormal response with BYM2 spatial effects, RW1/RW2 temporal effects, and structured interactions, it reveals nuanced patterns in cancer incidence. Our application to Iranian data demonstrates its superiority over standard models and provides actionable insights for public health policy and targeted prevention strategies.

Future research should extend the LNSTAR framework to district-level data, incorporate additional covariates, and investigate spatially varying coefficient models to further elucidate the factors underlying geographic heterogeneity in breast cancer incidence.

References

Baio, G. (2012). *Bayesian Methods in Health Economics*. CRC Chapman & Hall, London.

Berry, S., Carlin, B., Lee, J., and Muller, P. (2011). *Bayesian Adaptive Methods for Clinical Trials*. CRC Chapman & Hall, New York.

Besag, J.(1974). Spatial interaction and the statistical analysis of lattice systems. *Journal of the Royal Statistical Society: Series B (Methodological)*, **36**(2), 192-225.

Besag, J., and Kooperberg, C. (1995). On conditional and intrinsic autoregressions. *Biometrika*, **82**(4), 733-746.

Besag, J., York, J., and Mollie, A. (1991). Bayesian image restoration, with two applications in spatial statistics. *Annals of the Institute of Statistical Mathematics*, **43**(1), 1-20.

Blangiardo, M., and Cameletti, M. (2015). *Spatial and Spatio-Temporal Bayesian Models with R-INLA*. John Wiley & Sons, West Sussex, UK.

Blangiardo, M., Cameletti, M., Baio, G., and Rue, H. (2013). Spatial and spatio-temporal models with R-INLA. *Spatial and spatio-temporal epidemiology*, **7**, 39-55.

Cressie, N. (1993) *Statistics for Spatial Data*. John Wiley & Sons, Inc.

Cressie, N., and Chan, N.H. (1989). Spatial modeling of regional variables. *Journal of the American Statistical Association*, **84**(406), 393-401.

Cressie, N., and Wikle, C.K. (2011). *Statistics for Spatio-Temporal Data*. Wiley, Hoboken, NJ.

Fahrmeir, L., Kneib, T., and Lang, S. (2004). Penalized structured additive regression for space-time data: a Bayesian perspective. *Statistica Sinica*, **14**(3), 731-761.

Faramarzi, Sh., Kiani, B., Faramarzi, Sh, and Firouraghi, N. (2024). Cancer patterns in Iran: a gender specific spatial modelling of cancer incidence during 2014–2017. *BMC cancer*, **24**(1), 191.

Gelman, A., Lee, D., and Guo, J. (2015). Stan: a probabilistic programming language for Bayesian inference and optimization. *Journal of Education and Behavioral Statistics*, **40**(5), 530-543.

Gómez-Rubio, V. (2020). *Bayesian Inference with INLA*. CRC Press.

Greenland, S. (2006). Bayesian perspectives for epidemiological research: I. Foundations and basic methods. *International Journal of Epidemiology*, **35**(3), 765-775.

Hashemi, H., Mahaki, B, and Farnoosh, R. Comparing Spatial Ecological Regression Models in Breast Cancer Incidence in Iran. *Journal of Research and Health*, **14**(4), 329-340.

Knorr-Held, L. (2000). Bayesian modelling of inseparable space-time variation in disease risk. *Statistics in Medicine*, **19**(17-18), 2555-2567.

Lang, S., Kneib, T., and Brezger, A. (2005). BayesX: analyzing Bayesian structural additive regression models. *Journal of Statistical Software*, **14**(11), 1-22.

Li, Y., Brown, P., Rue, H., Al-Maini, M., and Fortin, P. (2012). Spatial modelling of lupus incidence over 40 years with changes in census areas. *Journal of the Royal Statistical Society Series C: Applied Statistics*, **61**(1), 99-115.

Luan, H., Quick, M., and Law, J. (2016). Analyzing local spatio-temporal patterns of police calls-for-service using Bayesian integrated nested Laplace approximation. *International Journal of Geo-Information*, **5**(9), 162.

Lunn, D., Spiegelhalter, D., Thomas, A., and Best, N. (2009). The BUGS project: Evolution, critique and future directions. *Statistics in Medicine*, **28**(25), 3049-3067.

Rahimzadeh, Sh., Bentham, J., Burczynska, B., Farzadfar, F, and Di Cesare, M. (2025). Spatiotemporal disparity of breast cancer incidence in Iranian female populations at the district level from 2000 to 2021: Bayesian disease mapping. *Plos one* , **20**(9), e0330017.

Riebler, A., Held, L., and Rue, H. (2012). Estimation and extrapolation of time trends in registry data-borrowing strength from related populations. *The Annals of Applied Statistics*, **6**(1), 304-333.

Riebler, A., Sørbye, S.H., Simpson, D., and Rue, H. (2016). An intuitive Bayesian spatial model for disease mapping that accounts for scaling. *Statistical Methods in Medical Research*, **25**(4), 1145-1165.

Rue, H., Martino, S., and Chopin, N. (2009). Approximate Bayesian inference for latent Gaussian models by using integrated nested Laplace approximations. *Journal of the Royal Statistical Society, Series B*, **71**(2), 319-392.

Simpson, D., Rue, H., Riebler, A., Martins, T.G., and Sørbye, S.H. (2017). Penalising model component complexity: A principled, practical approach to constructing priors. *Statistical Science*, **32**(1), 1-28.

Spiegelhalter, D.J., Best, N.G., Carlin, B.P., and Van Der Linde, A. (2002). Bayesian measures of model complexity and fit. *Journal of the Royal Statistical Society Series B: Statistical Methodology*, **64**(4), 583-639.

Utazi, E.C., Afuecheta, E.O., and Nnanatu, C.C. (2018). A Bayesian latent process spatio temporal regression model for areal count data. *Spatial and Spatio-Temporal Epidemiology*, **25**, 25-37.

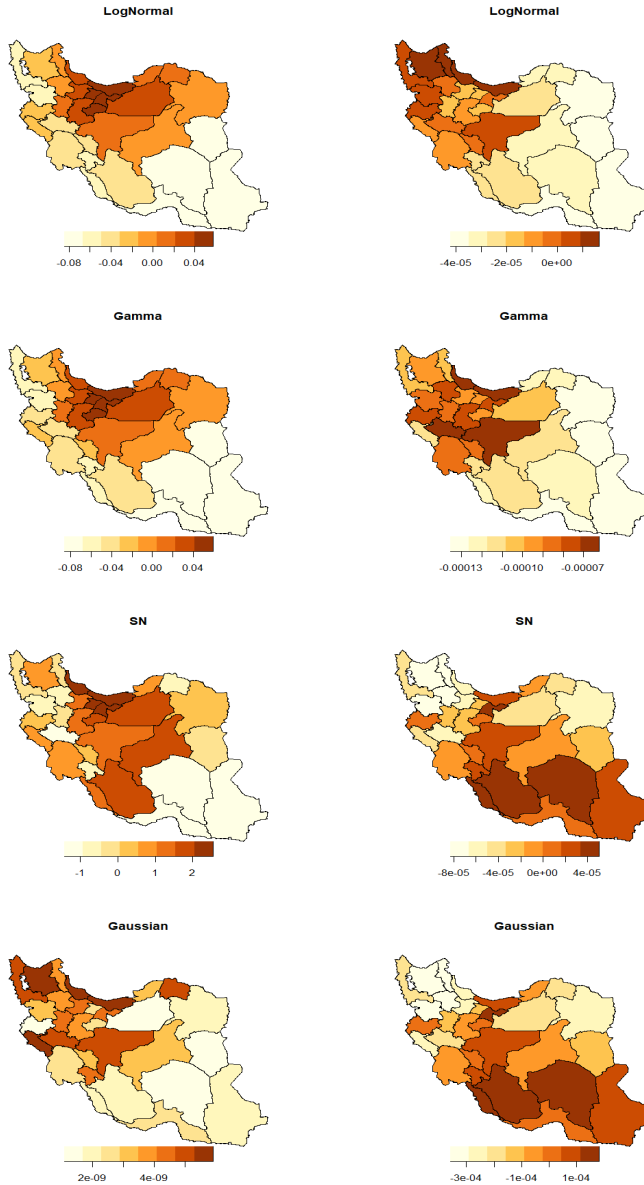

Figure 1: Bayes estimators of spatial effects for all models, comparing Type II (left column) and Type IV (right column) spatio-temporal interactions.

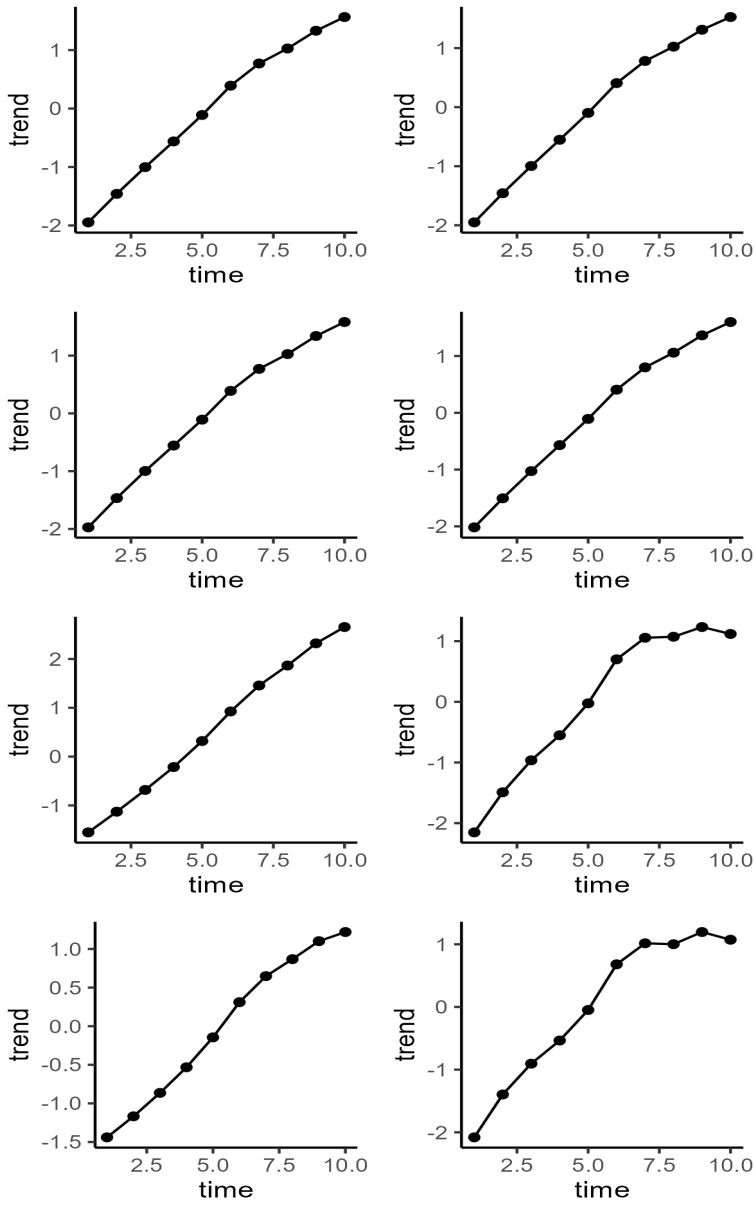

Figure 2: Bayes estimators of temporal effects for all models, comparing Type II (left column) and Type IV (right column) spatio-temporal interactions.

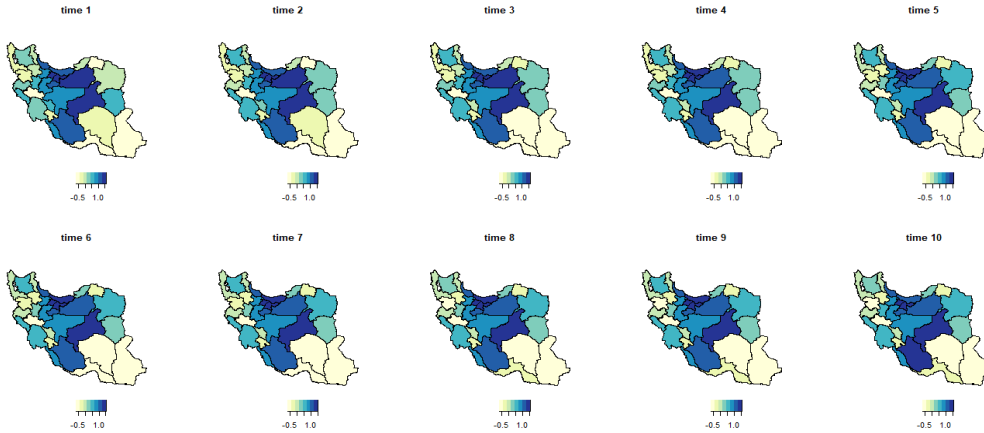

Figure 3: Bayes estimators of Type II spatio-temporal interactions in the LNSTAR model.

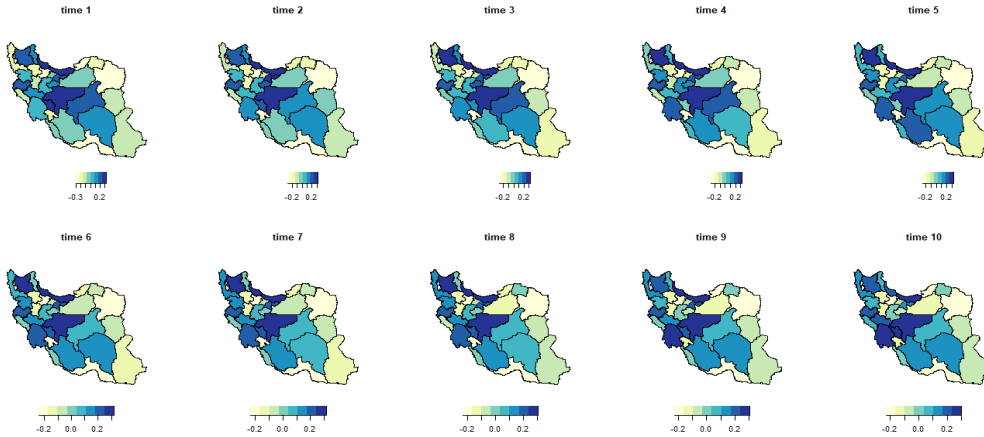

Figure 4: Bayes estimators of Type IV spatio-temporal interactions in the LNSTAR model.

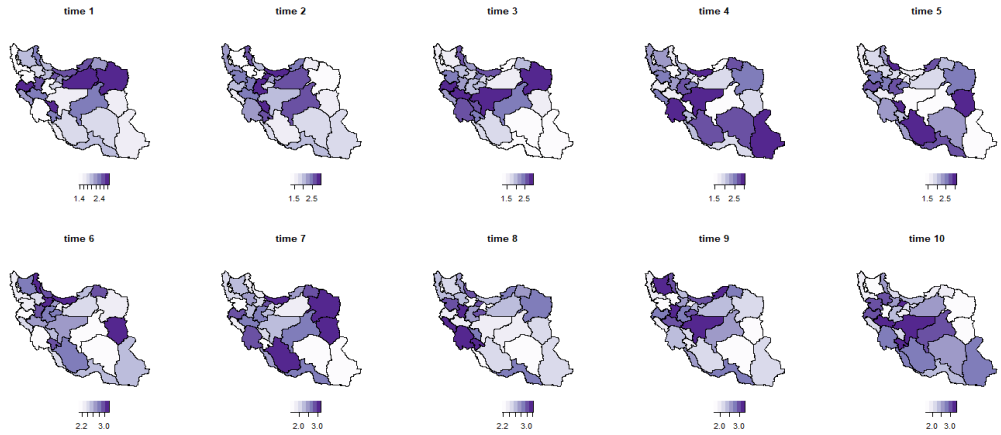

Figure 5: Bayes estimators of breast cancer incidence rates in the presence of Type II spatio-temporal interactions (LNSTAR model).

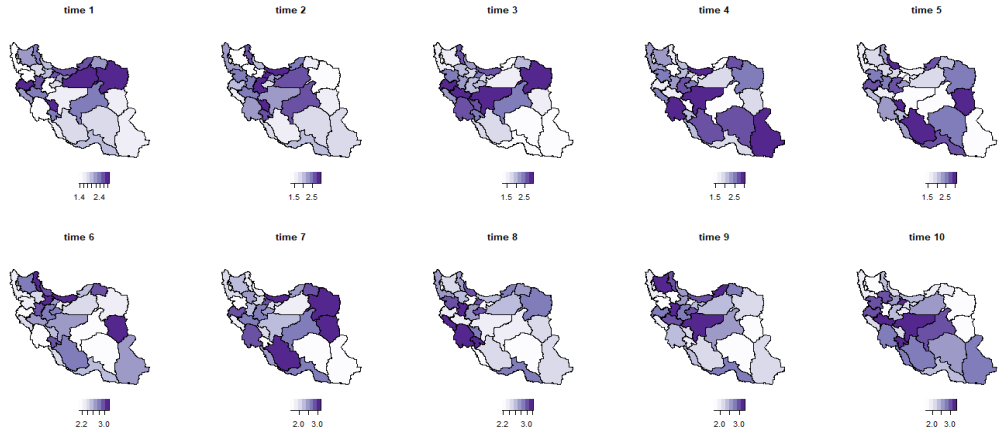

Figure 6: Bayes estimators of breast cancer incidence rates in the presence of Type IV spatio-temporal interactions (LNSTAR model).